

# Seismic Spectral Attributes using Coherence and Semblance Algorithms

Williams Ofuyah<sup>1\*</sup> Olatunbosun Alao<sup>2</sup> Victor Olaseni<sup>3</sup> Lukman Adeoti<sup>4</sup>

1.Department of Earth Sciences, Federal University of Petroleum Resources, Effurun, Nigeria

2.Department of Geology, Obafemi Awolowo University, Ile-Ife, Nigeria

3.Department of Physics, Federal University of Petroleum Resources, Effurun, Nigeria

4.Department of Geosciences, University of Lagos, Akoka, Lagos, Nigeria

\* E-mail of the corresponding author: [wnofuyah@yahoo.com](mailto:wnofuyah@yahoo.com)

## Abstract

Fault detection technologies such as coherency algorithms, and derivative methods which evolved recently have proven to be important tools for seismic interpretation. In this paper the results of the application of frequency-based semblance algorithm to imaging subtle geologic features such as micro faults, variation in stratigraphy, etc. in the interpretation of 3D seismic data from the Niger delta are presented. The semblance images seismic discontinuities by computing the ratio of the total energy of a stack of traces within a time gate to the sum of the energy of the component traces within the same gate. Spectral decomposition uses the discrete Fourier transform to image thickness variability within the window. The aim of this study was to develop a practical technique for mapping subtle stratigraphic units embedded within seismic volume and which are usually masked after normal data interpretation using semblance algorithms and spectral decomposition. The methodology combined conventional semblance techniques and non-conventional technique of the discrete Fourier transform within Matlab software. The geologic features were analyzed to include stratigraphic and near-vertical structural features by using a variable analysis window centered on the top of a conventionally interpreted thin sand interval along an arbitrary line. The line was drawn to connect the entire six wells in the seismic survey within Kingdom suite software. The transform attribute maps of response amplitude, phase and frequency of field Gamma-ray, seismic, and semblance data revealed fault and stratigraphic details and new prospects. The spectral semblance algorithm is valuable in mapping unfavourable geologic environments.

**Keywords:** Discrete Fourier transform, Coherence, Semblance, Spectral decomposition

## 1. Introduction

Fault detection technologies such as coherency algorithms, and derivative methods which evolved recently have proven to be important tools for seismic interpretation. In this paper, the results of the application of frequency-based semblance algorithms to imaging subtle geologic features such as micro-faults, variation in stratigraphy, etc. in the interpretation of 3D seismic data from the Niger delta are presented. The semblance images seismic discontinuities by computing the ratio of the total energy of a stack of traces within a time gate to the sum of the energy of the component traces within the same gate (Telford et al, 1985). Seismic coherency, also a measure of semblance, images discontinuities by calculating localized seismic trace similarity (Peyton et al, 1998). It measures lateral changes in the seismic response caused by variation in structure, stratigraphy, lithology, porosity, and the presence of hydrocarbons (Marfurt et al, 1998) within a narrow time gate. Among the several advantages offered by seismic coherency are the ability to carefully analyze structural and stratigraphic features over an entire data volume including zones that are shallow, deep and adjacent to the primary zone of interest, identify and interpret subtle feature that are not represent able by picks on peaks, troughs, or zero-crossings, generate paleo-environmental maps of channels and fans corresponding to sequence versus reflector boundaries, etc. (Marfurt et al 1998).

Spectral decomposition uses the discrete Fourier transform (DFT) to image thickness variability (Peyton et al, 1998). It provides a novel means of utilizing seismic data and DFT for imaging and mapping temporal bed thickness and geologic discontinuities over large 3D seismic surveys. By transforming the seismic data and its attributes into the frequency domain via the DFT, amplitude spectra delineate temporal bed thickness variability, while the phase spectra indicate lateral geologic discontinuities. This technology has delineated stratigraphic settings like channel sands and structural settings involving complex fault systems in 3D seismic surveys (Partyka et al., 1999)

The aim of this study was to develop a practical technique for mapping subtle stratigraphic units embedded within seismic volume and which are usually masked after normal data interpretation using semblance algorithms and spectral decomposition. The methodology combined conventional semblance techniques and non-conventional technique of the discrete Fourier transform within Matlab software. The geologic features were analyzed to include stratigraphic and near-vertical structural features by using a long and short analysis windows centered on the top of a conventionally interpreted thin sand interval along an arbitrary line. The line was drawn to connect the entire six well in the seismic survey within Kingdom suite software. The seismic coherency and

semblance was computed from an extracted data volume integrating the zone of interest along the arbitrary seismic line. This was followed by the transformation of the results obtained in time into frequency using the DFT and comparison of both results.

The transform attribute maps of response amplitude, phase and frequency of field Gamma-ray, measured seismic, and computed coherence and semblance data revealed fault and stratigraphic details and new prospects. The spectral semblance algorithm is valuable in mapping unfavourable geologic environments.

The main conclusion is that spectral decomposition of the conventionally computed coherence and semblance data enhances resolution capability resulting in better geologic maps. This has application in the localization of thin-bed reflections and definition of bed thickness variability within complex rock strata including the detection of subtle discontinuities like facies change, channels, microfaults, reflection-free events within large 3D volume.

The key inputs are the concepts and practices of seismic stratigraphy and principles of spectral decomposition and a clear knowledge of signal analysis and thin-bed tuning phenomena and properly migrated seismic data.

## 2. Field Description

The Niger delta is one of the most prolific oil producing areas in the world. It is located in southern Nigeria between latitudes 3<sup>0</sup>N and 6<sup>0</sup>N and longitudes 4<sup>0</sup>30<sup>1</sup> E and 9<sup>0</sup>E. The delta covers an area of about 105,000km<sup>2</sup>.

The Niger delta is a large arcuate delta of the destructive wave dominated type and is divided into the continental, transitional and marine environments. A sequence of under compacted marine shale (Akata formation, depth from 11121 ft) is overlain by paralic or sand/shale deposits (Agbada formation, depth from 7180-11121ft) is present throughout. Growth faults strongly influenced the sedimentation pattern and thickness distribution of sands and shales. The paralic interval is overlain by a varying thickness of continental sands (Benin formation, depth from 0-6000ft). Hydrocarbon is trapped in many different trap configurations. Oil and gas are trapped by roll-over anticlines and growth faults (Weber, 1987). Merki (1972) noted that the age of the formations become progressively younger in a down-dip direction and ranges from Paleocene to Recent.

### 2.1 Seismic Data

The seismic data used in this study are digital and real. The recorded data sets (3D) were obtained over 'X' field by Chevron Corporation Nigeria. The field data comprises a base map, a suite of logs from six (6) wells, and four hundred (400) seismic lines and 220 crosslines. Some of the log types provided are Gamma-ray (GR), self-potential, resistivity density, sonic, water saturation.

## 3. Seismic Coherence

Coherence is a measure of the similarity between waveforms or Seismic traces. Coherence is defined as energy ratio which is normalized by total energy of the trace within the calculation window. For a large number of seismic traces, we could use the fact that when we stack several channels together, the resulting amplitude is generally large where the individual channels are similar (coherent) so that they stack in-phase, and small where they are unlike (incoherent). The ratio of the energy of the stack compared to the sum of the energies of the individual components is a measure of the degree of coherence expressed as:

$$\text{Coherence, } E_c = \frac{(\sum_i x_{it})^2}{\sum_i (x_{it}^2)} \quad (1)$$

where

$x_{it}$  is the amplitude of the individual channel  $i$  at the time  $t$ .

$\sum_i x_{it}$  is the amplitude of the stack at time  $t$  and the square of this will be the energy.  $E_c$  is the ratio of the output energy to the sum of the energies of the input traces.

The coherence algorithm attribute is designed to emphasize discontinuous events such as faults. Coherent event is expected to extend over a time interval with a high amplitude value on this attribute corresponding to discontinuities in the data, while a low amplitude value corresponds to continuous features.

## 4. Semblance

This edge detection attribute is a more meaningful quantity than the coherence attributes ( $E_c$ ) which measures edges over a narrow window. According to Tanner et al. (1979), semblance ( $S_c$ ) denotes the ratio of the total energy of the stack, within a gate of length  $\Delta t$ , to the sum of the energy of the component traces within the same time gate. Using the same terminology as before we can write semblance as

$$S_c = \frac{\sum_{t=t_1}^{t_2} (\sum_i x_{it})^2}{\sum_{t=t_1}^{t_2} \sum_i (x_{it}^2)} \quad (2)$$

The semblance attribute will not only tend to be large when a coherent event is present but the magnitude of the semblance will also be sensitive to the amplitude of the event. Thus strong events usually

exhibit large semblance and weak events will exhibit moderate values of semblance while incoherent data will have very low semblance. (Taner et al., 2009).

## 5. Discrete Fourier Transform (DFT)

The Discrete Fourier Transform (DFT) is the digital equivalent of the continuous Fourier transform and is expressed as

$$f(w) = \sum f(t) e^{-iwt} \quad (2)$$

where,  $w$  is the Fourier dual of the variable 't'. If 't' signifies time, then 'w' is the angular frequency which is related to the linear (temporal) frequency 'f'. Also,  $F(w)$  comprises both real ( $F_r(w)$ ) and imaginary  $F_i(w)$  components. (Yilmaz, 2001).

## 6. Method

The main objective of our study was to develop a practical technique for mapping subtle stratigraphic units which are usually masked after normal data interpretation using the edge detection techniques of coherence and semblance. These have the advantage of acting solely on the seismic data and are therefore devoid of horizon picker biases. The methodology combined conventional semblance algorithms and non-conventional technique of the discrete Fourier transform within Matlab software. The geologic features were analyzed to include stratigraphic and near-vertical structural features by using separately, short (coherence) and long (semblance) analysis windows centered on the top of a conventionally interpreted thin sand interval along an arbitrary line. The line was drawn to connect the entire six wells in the seismic survey within Kingdom suite software. The transform attribute maps of response amplitude, phase and frequency of field Gamma-ray, seismic, coherence and semblance data were plotted afterwards.

## 7. Discussion of Results

The results obtained are displayed as Figures 1 to 3. Figure 1 shows the amplitude and phase spectral plots by DFT using different analysis window centered at top of a sand interval (2.752 seconds): (a) GR at 2.752s.

Original amplitude at 2.752s (c) coherence (short window centered at 2.752s) (d) semblance (long window centered at 2.752s) to integrate stratigraphic and near structural features. Note the change in phase direction here. The magnitude plot is perfectly symmetrical about the Nyquist frequency of 50Hz. The useful information in the signal is found in the range 0-50Hz. There is close resemblance of the edges at the 30 and 60Hz locations (i.e. F1, F2 on seismic section) in GR and coherence phase plots than on field data. The implication of this is that properly processed remotely sensed field data like seismic can approximate well or in-situ data.

Figure 2 is an integrated display of time and frequency attributes of GR, original seismic amplitude and coherence maps in the following order: (i) Gamma-ray amplitude time map and its corresponding frequency maps (b-e) and (ii) Amplitude map(a, f) and its corresponding coherence maps (g-j). Note the low GR amplitude and frequency values at the good well locations (green-orange). There is better edge definition at **B** (coherence) than at **A** (amplitude). The stratigraphic and structural elements are more evident in the coherence maps than on the original amplitude data.

The shale lineation (light blue, high frequency) straddling the low frequency sand zone (green, yellow and orange) are better delineated in (c) (circled). The good well locations in the field data are the orange and brown segments (d), detailed analysis indicate that wells 2, 3 and 6 were sited on sand/shale interface. However the green location in (d) is a prospective zone by its low frequency anomaly.

Figure 3 shows (i) Gamma-ray amplitude time slice (b-e) and its corresponding frequency slices and (ii) Amplitude slice (a, f) and its corresponding semblance time and frequency slices (g-j). Note the low GR amplitude and frequency values at the good well locations. Better edge definition at **D** (semblance) than at **C** (amplitude). The structural elements are more evident on semblance than on the coherence maps. The GR maps are displayed for identifying sand/shale location in relation to the computed frequency attributes.

The coherence maps highlight the discontinuous events or edges such as faults. High amplitude values of coherence correspond to discontinuities in the data, while low amplitude values correspond to continuous features. Figure 3f is the amplitude (time) slice and Figures 3g-j are the corresponding discontinuity time and frequency slices. Note that structural elements like faults were clearly unmasked in the discontinuity slices (e.g. Figure 3g along the vertical axis of well 01).

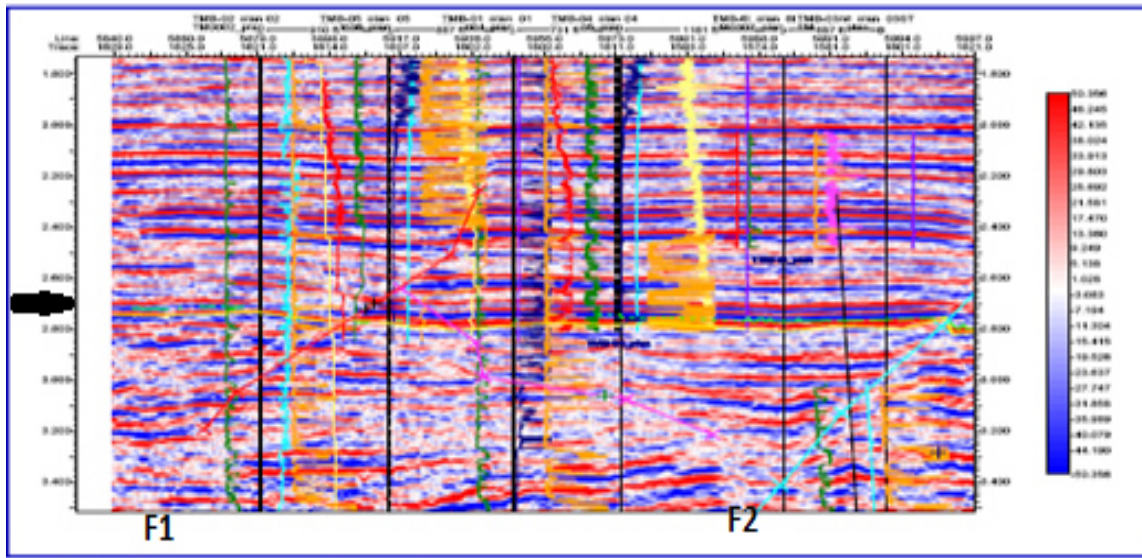
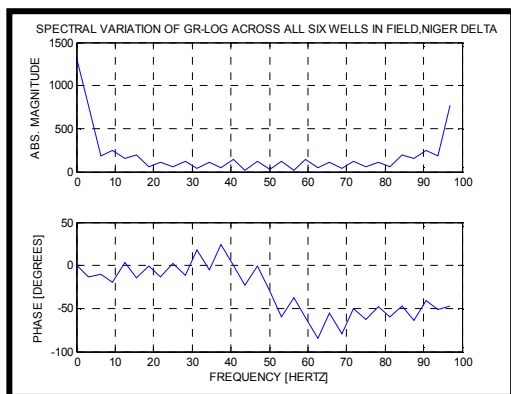
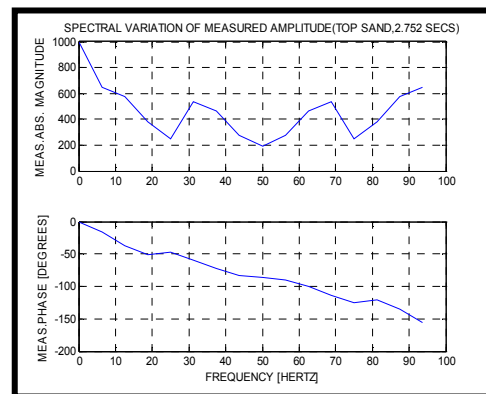


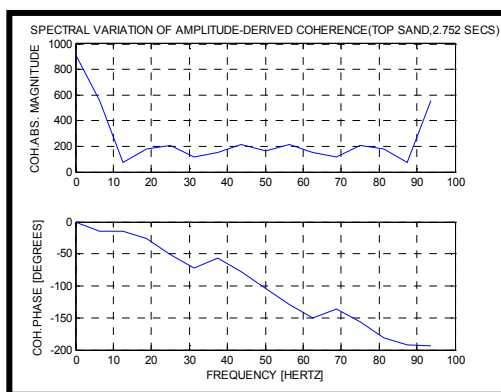
Figure 1. Arbitrary line after interpretation: Two major faults, F1, F2 are shown bounding the wells at the reservoir interval under analysis (2.752-2.768 secs, arrowed).The well locations are indicated above the seismic section



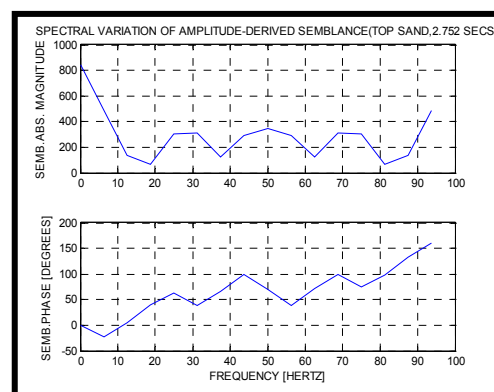
(a) Spectra of Gamma –Ray log across wells.



(b) Spectra of Measured Amplitude



(c) Spectra of Amplitude-Derived Coherence



(d) Spectra of Amplitude-Derived Semblance

Figure 2. Amplitude and phase Spectral plots by DFT using different analysis window at and centered at top of sand interval (2.752 seconds): (a) GR at 2.752s. (Note the phase reversal). (b) Original amplitude at 2.752s (c) coherence (short window centered at 2.752s) (d) semblance (long window centered at 2.752s to intergrate

Figure 2: Amplitude and phase Spectral plots by DFT using different analysis window at and centered at top of sand interval (2.752 seconds): (a) GR at 2.752s.(Note the phase reversal) (b) Original amplitude at 2.752s (c) coherence (short window centered at 2.752s) (d) semblance (long window centered at 2.752s to intergrate



stratigraphic and near structural features. Note the change in phase direction). The magnitude plot is perfectly symmetrical about the Nyquist frequency of 50Hz. The useful information in the signal is found in the range 0-50Hz. Compare the close resemblance of the edges at the 30 and 60Hz locations (i.e. F1, F2 on seismic section) in GR and coherence than in field data.

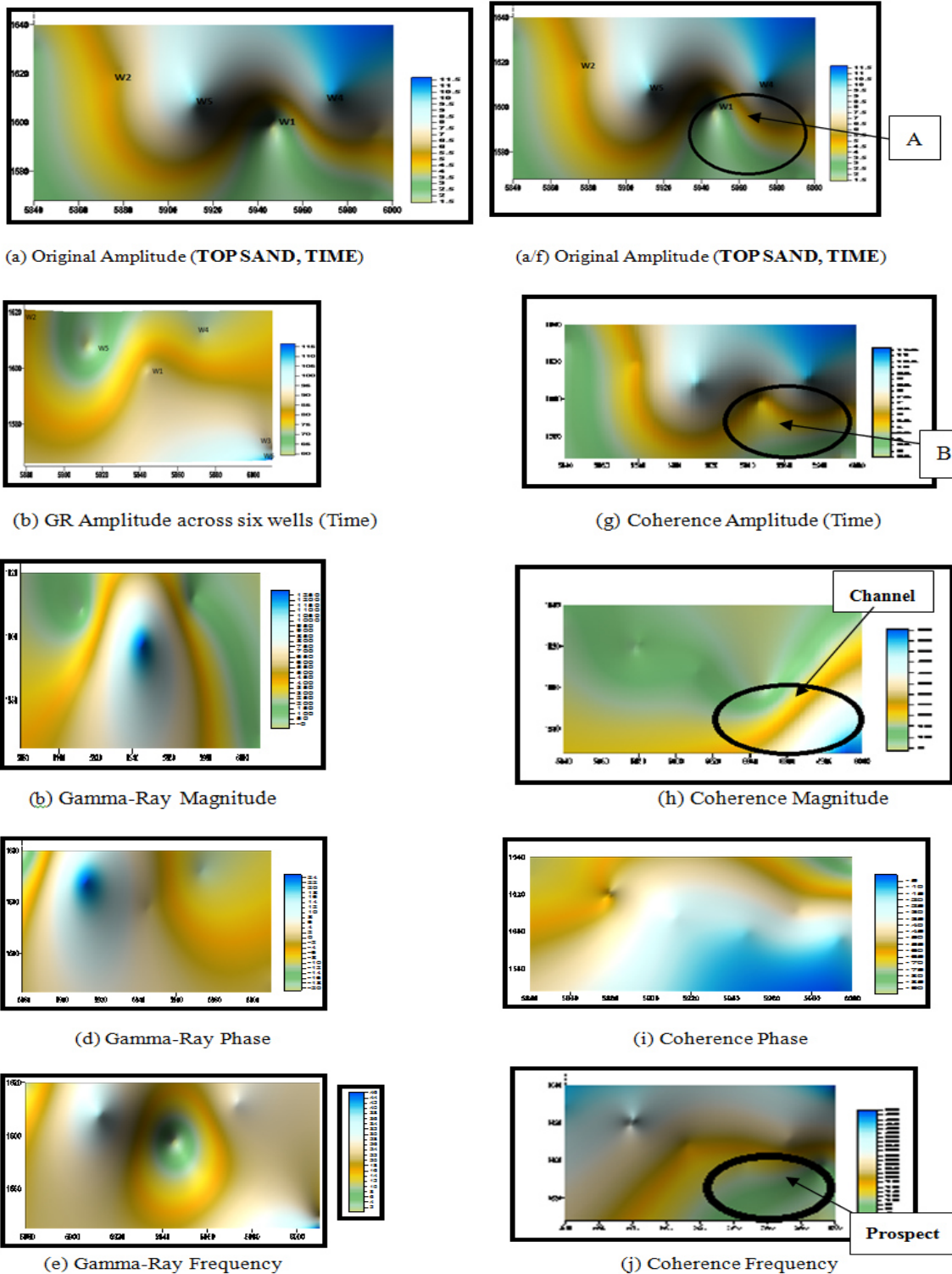


Figure 3. Top of sand (2.752 seconds): (i) Gamma-ray amplitude time map and its corresponding frequency maps (b-e) and (ii) Amplitude map (a, f) and its corresponding coherence maps (g-j). Note the low GR amplitude and frequency values at the good well locations (green-orange). There is better edge definition at B (coherence) than at A (amplitude).

Figure 3. Top of sand (2.752 seconds): (i) Gamma-ray amplitude time map and its corresponding

frequency maps (b-e) and (ii) Amplitude map(a, f) and its corresponding coherence maps (g-j). Note the low GR amplitude and frequency values at the good well locations (green-orange). There is better edge definition at B (coherence) than at A (amplitude). The stratigraphic and structural elements are more evident in the coherence maps than on the original amplitude data.

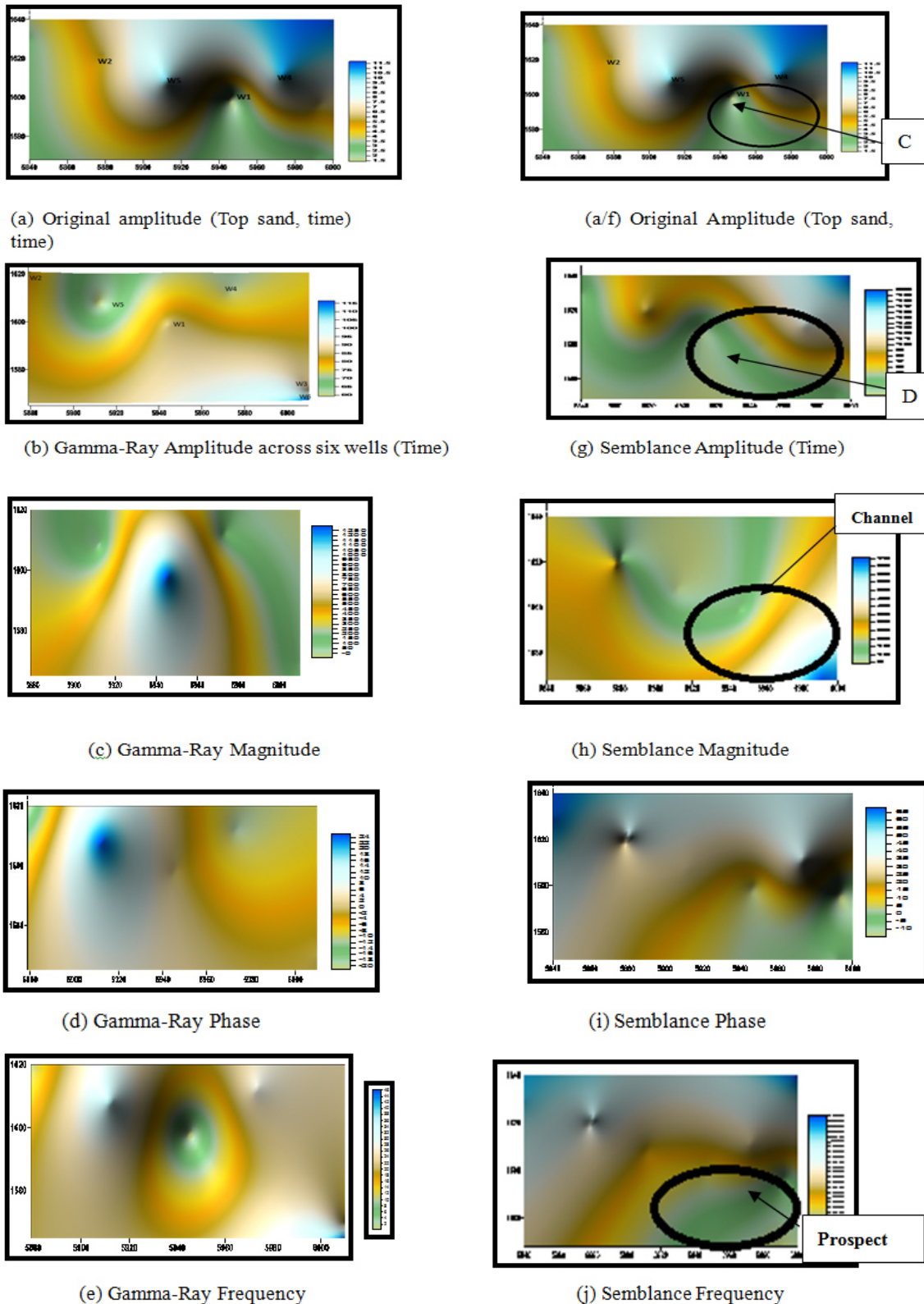


Figure 4. Top of sand (2.752 seconds) (i) Gamma-ray amplitude time slice (b-e) and its corresponding frequency slices and (ii) Amplitude slice (a, f) its corresponding semblance time and frequency slices (g-j).

Figure 4: Top of sand (2.752 seconds) (i) Gamma-ray amplitude time slice (b-e) and its corresponding

frequency slices and (ii) Amplitude slice (a, f) its corresponding semblance time and frequency slices (g-j). Note the low GR amplitude and frequency values at the good well locations. Better edge definition at D (semblance) than at C (amplitude). The structural elements are more evident on semblance than on the coherence maps. The GR maps are for sand/shale location in relation to the computed frequency attributes.

Coherence magnitude map (Figure 3h) highlights the main seismic features and represents the acoustic impedance contrast. It also reveals edges, changes in lithology, faults, and changes in deposition and sequence boundaries. Figure 3i shows the map of coherence phase. This indicates lateral continuity or sequence boundaries and also facilitates visualization of bedding discontinuities. The coherence frequency map (Figure 3j) shows the drilled hydrocarbon zones and potential prospects areas by its low frequency anomaly. Higher frequencies indicate sharp discontinuities or thin shale.

In Figure 4, Top of sand (2.752 seconds) the order of display is (i) Gamma-ray amplitude time slice (b-e) and its corresponding frequency slices and (ii) Amplitude slice(a, f) its corresponding semblance time and frequency slices (g-j). Note the low GR amplitude and frequency values at the good well locations. Better edge definition at **D** (semblance) than at C (amplitude). The structural elements are more evident on semblance than on the coherence maps. Here large semblance values show strong events while weak events have moderate values of semblance. The zones with very low semblance values are the incoherent events.

## Conclusions

We have investigated the resolving capacity of the coherence and semblance attributes computed in terms of energy ratio of traces within narrow and wide windows respectively in time domain and the corresponding response attributes in frequency domain using the discrete Fourier transform for the determination of lateral relations in our data. The main objective of our study was to develop a robust technique for mapping subtle stratigraphic units which are usually masked after normal data interpretation using the edge detection techniques of semblance algorithms which act on the seismic data and is devoid of horizon picker biases. Our approach reveals that computing a suite of coherence and semblance attributes in frequency domain rather than relying on visualization of faults and channels from horizon picks gives better results. The structural and stratigraphic elements are more evident on semblance than on the coherence maps.

The spectral coherency and semblance adopted gave improved geologic maps. The outputs of the algorithm revealed sub-seismic faults, discontinuities, channel, and amplitude / petrophysical parameter transforms of the field. The reliability of the result is reinforced by its good correlation with Gamma-ray and other log data. This has application in the localization of thin-bed reflections and definition of bed thickness variability within complex rock strata including the detection of subtle discontinuities like facies change, channels, microfaults, reflection-free events within large 3D volume. It is hoped that future work would adopt more sophisticated signal transforms owing to the windowing limitations of the discrete Fourier transform.

## Acknowledgements

The authors thank Chevron Corporation, Nigeria for making the seismic and well data available for use. We are indebted to Shell Nigeria for the use of the Kingdom Suite Software at its work station at Department of Geology, Obafemi Awolowo University (O.A.U.), Ile-Ife, Nigeria and the Federal University of Petroleum Resources, Effurun, Nigeria for the use of her computing facilities.

## References

- Marfurt, K.J.; Sharp, J.A.; Scheet, R.M.; Ward, J., Cain, C and Harper, M.G. (1998), "Suppression of the acquisition footprint for seismic attribute analysis", *Geophysics*, 68, pp. 1024-1035.
- Merki, P. J. (1972), "Structural Geology of the Cenozoic Niger Delta", In: Dessauvague, T. F. J. and Whiteman, A. J. (eds), African Geology, University of Ibadan Press, Nigeria. pp. 635-646.
- Partyka, G.A., Gridley, J.M. and Lopez, J. (1999), "Interpretational Applications of Spectral Decomposition in Reservoir Characterization", *The Leading Edge*, 18(3): 353-360.
- Taner, M.T., Koehler and Sheriff, R.E. (1979), "Complex Trace Analysis", *Geophysics*, (44): 1041 – 1063. Revisited, 64th Annual International Meeting, SEG, Expanded Abstracts, 1104–1106.
- Telford, W. M.; Geldart, L.P.; Sheriff, R.E. and Keys, D.A. (1985), "Applied Geophysics", pp. 393-396, Cambridge University Press.
- Peyton, L., Bottjer, R. and Partyka, G., (1998), "Interpretation of incised valleys using new 3-D seismic techniques: A case history using spectral decomposition and coherency", *The leading Edge*, 17, 1294-1298.
- Weber, K.J. (1987), "Hydrocarbon Distribution Patterns in Nigerian Growth Fault Structures Controlled by Structural Style and Stratigraphy", *Journal of Petroleum Science and Engineering*, 1: 91-104.
- Yilmaz O., (2001), "Seismic Data Analysis: Processing, Inversion, and Interpretation of Seismic Data": Society of Exploration Geophysicists, 2027 p.

The IISTE is a pioneer in the Open-Access hosting service and academic event management. The aim of the firm is Accelerating Global Knowledge Sharing.

More information about the firm can be found on the homepage:  
<http://www.iiste.org>

## CALL FOR JOURNAL PAPERS

There are more than 30 peer-reviewed academic journals hosted under the hosting platform.

**Prospective authors of journals can find the submission instruction on the following page:** <http://www.iiste.org/journals/> All the journals articles are available online to the readers all over the world without financial, legal, or technical barriers other than those inseparable from gaining access to the internet itself. Paper version of the journals is also available upon request of readers and authors.

## MORE RESOURCES

Book publication information: <http://www.iiste.org/book/>

## IISTE Knowledge Sharing Partners

EBSCO, Index Copernicus, Ulrich's Periodicals Directory, JournalTOCS, PKP Open Archives Harvester, Bielefeld Academic Search Engine, Elektronische Zeitschriftenbibliothek EZB, Open J-Gate, OCLC WorldCat, Universe Digital Library, NewJour, Google Scholar

